



# Development of forming limit diagrams for motorcycle fuel tank made from AA5754-O under deep drawing

Phiraphong LARPPRASOETKUN<sup>1</sup>, Jidapa LEELASEAT<sup>1</sup>, Aeksuwat NAKWATTANASET<sup>1</sup> and Surasak SURANUNTCHAI<sup>1,\*</sup>

<sup>1</sup> King Mongkut's University of Technology Thonburi, 126 Pracha Uthit Rd., Bang Mod, Thung Khru, Bangkok 10140, Thailand

\*Corresponding author e-mail: surasak.sur@kmutt.ac.th

**Received date:**  
26 March 2024  
**Revised date:**  
17 June 2024  
**Accepted date:**  
5 July 2024

## Keywords:

Forming limit curve;  
Laser marking combined  
with elastic paints;  
Keeler-Brazier modified I

## Abstract

The research studied forming limit curves (FLC) for aluminum alloy 5754-O (AA5754-O) and modified them using two methods. These methods aimed to create FLCs for application in describing the forming behavior of sheet metal material through a deep drawing process simulation in the PAM-STAMP program. The methods are as follows: The Nakajima test combined with a new method, a novel process for grid creation on the specimen: laser marking combined with elastic paints. A mathematical material model using the fracture model along with the yield criteria: YLD2000-2D and hardening law: Swift-Voce. The Keeler-Brazier modified equation was chosen as the fracture model for this research because it is an effective equation for creating FLCs for steel materials and has not yet been applied to aluminum materials. Furthermore, no one has previously used the Keeler-Brazier modified equation in conjunction with YLD2000-2D and the yield criterion Swift-Voce hardening law. In summary, the FLC generated from YLD2000-2D, Swift-Voce hardening law, and Keeler-Brazier modified equations can predict the location of damage occurrence on the motorcycle fuel tank, which occurs due to the deep drawing process, using finite element simulation accurately. This closely resembles the actual forming process in the industry.

## 1. Introduction

Nowadays, the automotive parts manufacturing industry seeks materials to reduce motorcycle weight [1], leading to lower fuel consumption and reduced environmental pollution [2]. However, these new materials must also possess strength comparable to steel. Aluminum alloy is the answer, with AA5754-O offering a lightweight solution. This aluminum alloy boasts a higher strength-to-weight ratio compared to conventional steel [3]. One of the motorcycle parts that can significantly reduce overall weight is the fuel tank. The deep drawing process, which typically involves components like the punch, die, and blank holder, is crucial for fuel tank production. This widely used technique is prevalent in current automotive component manufacturing. However, as the industry demands increasingly complex part geometries, challenges like material tearing, cracking, or thinning can arise during the sheet metal forming process. To address these challenges, manufacturers often employ simulation tools and Forming Limit Curve (FLC) analysis. These tools are used either preemptively, to predict the forming capabilities of the sheet metal before actual production, or reactively, to troubleshoot and improve production after encountering issues. Simulation tools allow engineers to virtually test different parameters such as material properties, tooling designs, and process conditions, ensuring that potential forming problems are identified and mitigated early on. FLC analysis, on the other hand, involves experimental or simulated data to establish the limits of strain beyond which material

failure (such as tearing or fracture) is likely to occur during forming. By utilizing FLC, engineers can establish safe forming limits for the material, guiding the design of the deep drawing process to prevent defects and ensure the quality of the final automotive components, such as motorcycle fuel tanks. For the material AA5754-O, a new lightweight material, continuous studies have been conducted by researchers. Notable studies on the FLC of AA5754-O include those by Bolin Ma in 2023 [4] and Q Hu in 2020 [5]. Additionally, research on the deep drawing process of AA5754-O has been conducted by Mevlut Turkoz in 2020 [6] and Tinkir in 2015 [7]. However, no researcher has studied the application of FLC from material models to predict damage locations on parts produced in the automotive manufacturing industry. This research aims to apply FLC to predict the formability of motorcycle fuel tank parts through simulation by finite element analysis in the PAM-STAMP program. Hence, this research aims to study forming limit curve and predict the damage to motorcycle fuel tanks manufactured from AA5754-O material during the deep drawing process with experimental data from laboratory tests and applying the conclusions to the automotive parts manufacturing industry of the country. Introducing new types of metal sheet materials into the automotive industry poses challenges in manufacturing without causing damage to the products. One tool that can assist the automotive industry in predicting the formability of metal sheet materials is the forming limit curve [8-10]. It can predict the material's behavior during the forming process and anticipate locations where damage

or cracks may occur on the products after forming [11,12]. FLC can be obtained through two methods: Nakajima stretch forming test and mathematical models/materials model. For Nakajima testing according to ISO 12004 [13], gridlines need to be created on the workpiece before testing. The most used method for creating gridlines is "Electrolyte etching" [14,15]. However, since it is not feasible to etch gridlines on materials in the aluminum alloy group by electrolyte etching, a new method has been proposed in this research: "Laser marking combined with elastic paints". This method allows for the creation of gridlines on AA5754-O material without affecting its mechanical properties. Due to the review of literature [16], various ideas have been proposed for creating grids on pieces that cannot be produced using "Electrolyte etching processes". For instance, direct laser ablation on the specimen to generate grid lines has been suggested. However, this method leaves traces of the laser, resulting in subsequent errors during testing. Moreover, direct laser application on the specimen also causes initial cracking, affecting the Nakajima testing outcomes. Therefore, researchers have developed a new method named "Laser marking combined with elastic paints." This method is employed to create grids on materials within the aluminum alloy group. Unlike direct laser application on the surface, this approach involves spraying black elastic rubberized peelable paint from Thailand onto the specimen before laser processing. Subsequently, the laser is used to remove the unwanted color, leaving behind only the desired grid lines on the specimen surface. Importantly, the laser used for grid marking does not directly contact the material, thus preserving the mechanical properties of the material. As for constructing the forming limit curve from mathematical models [17-20], numerous proposals and mathematical equations have been put forth by various individuals. The first person to propose the FLC was Keeler, and his equation is referred to as the Keeler Equation [21]. The Keeler equation has been widely adopted and continuously developed, resulting in several name changes over time. In this research, the Keeler-Brazier modified I [22] was selected to construct the FLC. These equations were utilized to predict the behavior of sheet metal materials during forming processes, including predicting areas where damage or cracking might occur on the final products following the deep drawing process of automotive parts are motorcycle fuel tank components. The Keeler-Brazier modified I equation was developed from the Keeler Equation by Paul in 2015 [23]. It considers the strain hardening coefficient ( $n$ ) and sheet thickness ( $t$ ) of the sheet metal material used in the manufacturing process. These parameters are utilized to calculate the minimum point on the forming limit curve, which is referred to as FLC<sub>0</sub>. FLC<sub>0</sub> is of great significance as it is needed to compute both the left side of the FLC and the right side of FLC<sub>0</sub>. In this research, the aim is to study and construct forming limit curves to assess the formability of sheet metal materials and predict the position where failure [24] will occur on the automotive part after the forming process [25]. The sheet metal materials used in the industry

must undergo a reduction process to achieve the desired thickness before being formed into products using various processes. Due to the reduction process thickness of the material sheet by the cold rolling process, the sheet metal materials had different mechanical properties in each direction relative to the rolling direction, leading to anisotropic behavior. Therefore, it is necessary to consider anisotropy in materials when constructing FLCs from material models. From the above analysis, the use of different material fracture criteria influences the FLC. In this research, for the aluminum alloy grade AA5754-O with a thickness of 1.5 mm used in the industry, its plastic-anisotropic behavior has not been verified using theoretical methods and experimental procedures in the laboratory. Therefore, the initial phase of this study involved conducting uniaxial tensile tests on the material to determine its mechanical properties, identifying the necessary parameters for the material fracture criteria, and conducting Nakajima stretch forming tests to obtain FLCs from experimental data for comparison with FLCs obtained from mathematical models studied. Hence, the study must consider and select yield criteria for investigation, namely the Hill 1948 (plane stress) yield criterion [26], the Barlat 1989 yield criterion [27] and YLD2000-2D yield criterion [28] combined with the Swift-Voce hardening law [29,30] because the Swift-Voce hardening law is commonly used for fitting material stress-strain curves in the aluminum alloy group [31,32]. Subsequently, the generated forming limit curve from the Keeler-Brazier modified I Equation, aims to achieve an accurate FLC closely based on the Nakajima stretch forming test. Finally, we will use the FLCs from Nakajima stretch forming tests and FLCs generated by mathematical models to compare predicted damage positions on workpieces after deep drawing process simulation by PAM-STAMP software with actual production in the automotive parts manufacturing industry for the fuel tank of motorcycle.

## 2. Experimental

### 2.1. Material testing of the aluminum alloy grade AA5754-O sheet

#### 2.1.1 Uniaxial tensile test

The uniaxial tensile test for the aluminum alloy grade AA5754-O material with a thickness of 1.5 mm can be prepared according to ASTM E8 [33] standards. In this research, test specimens are prepared at angles of 0, 45, and 90 degrees relative to the rolling direction of the aluminum alloy sheet to obtain the  $r$ -values [34,35], which indicates material anisotropy. The specimens are tested using a universal tensile testing machine at a constant strain rate of  $0.001 \text{ s}^{-1}$  until failure occurs. After the test, the true stress-strain curve and material mechanical properties are obtained, as shown in Table 1.

**Table 1.** Mechanical properties of AA5754-O in each rolling direction.

Rolling direction (degree)	Yield stress (MPa)	Ultimate tensile stress (MPa)	% Elongation	r-value
0	100.17	207.64	21.87440	0.5682
45	100.77	200.54	28.19605	0.7980
90	99.82	201.64	25.39769	0.6781

## 2.2.2 Nakajima stretch forming test

The Nakajima stretch forming test is conducted to obtain the forming limit curve. For this research, test specimens are prepared according to ISO12004 standards [13], where each specimen has a different shape as depicted in Figure 1(b), indicating a different form of strain due to the material receiving a different form of stress. After preparing the specimens, they are subjected to testing using an erichsen machine with a punch diameter of 100 mm. Once the testing of the specimens is complete, the true major strain and true minor strains are measured using an optical strain measurement system model AutoGrid Vialux. After measuring the strain values on the specimens, it can select the data from the area of the specimen that interests and plot the data for generated to obtain the forming limit curve. The universal sheet metal testing machine, also known as the erichsen machine, in this research setup can exert a maximum force of 400 kN for clamping the sheet metal, and a maximum force of 225 kN for holding it. The punch velocity used for the Nakajima test ranges from  $0.5 \text{ mm}\cdot\text{s}^{-1}$  to  $2 \text{ mm}\cdot\text{s}^{-1}$ . The Erichsen machine consists of a hemispherical punch with a diameter of 100 mm, a blank holder force, and a draw section with a diameter of 10 mm, as illustrated in Figure 1(a) of the research document.

## 2.3 Mathematical modelling of plasticity and fracture

### 2.3.1 Anisotropic yield models

#### 2.3.1.1 Hill's 1948 yield criterion

In considering metal sheet materials processed through cold rolling, the material exhibits anisotropic behavior. According to Hill's yield criterion theory, it is assumed that the sheet material is homogeneous and isotropic. The yield criteria by Hill are expressed as follows:

$$2f(\sigma) = F(\sigma_{xx} - \sigma_{yy})^2 + G(\sigma_{zz} - \sigma_{xx})^2 + G(\sigma_{zz} - \sigma_{yy})^2 - 2(L\sigma_{yz}^2 + M\sigma_{zx}^2 + N\sigma_{xy}^2) = 1 \quad (1)$$

In this research, considering the case of plane stress where  $\sigma_{xx} = \sigma_{yy} = \sigma_{zz} = 0$ , it can obtain Hill's 1948 yield criterion Equation as follows:

$$2f(\sigma) = (G+H)\sigma_{xx}^2 + (F+H)\sigma_{yy}^2 - 2H\sigma_{xx}\sigma_{yy} + 2N\sigma_{xy}^2 = 1 \quad (2)$$

Where,  $\sigma_{xx}$ ,  $\sigma_{yy}$  and  $\sigma_{zz}$  represent the stresses in the rolling (x-axis), transverse (y-axis), and thickness (z-axis) directions, respectively. The  $\sigma_{xy}$ ,  $\sigma_{yz}$  and  $\sigma_{zx}$  represent the shear stresses in the xy, yz, and zx planes, respectively. The variables F, G, H and N represent the isotropic constants of each direction, which can be obtained from the r-values obtained from tensile testing as follows:

$$F = \frac{r_0}{r_{90}(1+r_{90})}, G = \frac{1}{(1+r_0)}, H = \frac{r_0}{(1+r_0)}, N = \frac{(r_0+r_{90})(1+2r_{45})}{2r_{90}(1+r_0)} \quad (3)$$

Hill's 1948 R-anisotropic coefficients can be computed using the r-values of the specimens at  $0^\circ$ ,  $45^\circ$ , and  $90^\circ$  angles with respect to the rolling direction that were found by tensile testing, as indicated in Table 2.

#### 2.3.1.2 Barlat 1989 yield criterion

In 1989, Barlat and Lian developed the yield criteria function as follows:

$$F = a|k_1 + k_2|^M + b|k_1 - k_2|^M + c|2k_2|^M = 2\sigma_e^M \quad (4)$$

When M is the crystallographic structure of the material, for BCC, M = 6, and for FCC, M = 8. Where  $k_1$  and  $k_2$  are coefficients as following.

$$k_1 = \frac{\sigma_{11} + h\sigma_{22}}{2}; k_2 = \left[ \left( \frac{\sigma_{11} - h\sigma_{22}}{2} \right)^2 + p^2\sigma_{12}^2 \right]^{1/2} \quad (5)$$

The parameters a, c, h and p are materials parameter, for anisotropic materials can identified by Equation (6).

$$a = 2 - c = 2 - 2\sqrt{\frac{r_0}{1+r_0} \times \frac{r_{90}}{1+r_{90}}}, h = \sqrt{\frac{r_0}{1+r_0} \times \frac{1+r_{90}}{r_{90}}} \quad (6)$$

$$\text{and } p = \frac{\sigma_e}{\tau_{s1}} \left( \frac{2}{2a+2^M c} \right)^{1/M}$$

Barlat 1989 coefficients can be computed using the r-values of the specimens at  $0^\circ$  and  $90^\circ$  angles with respect to the rolling direction as indicated in Table 3

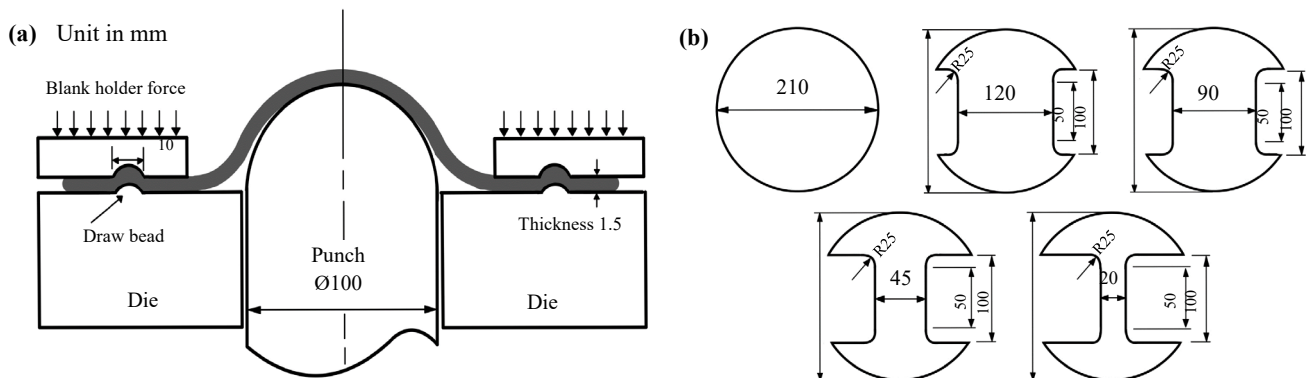


Figure 1. (a) Diagrammatic of the Nakajima test with punch diameter 100 mm, and (b) Drawing specimen of Nakajima test.

**Table 2.** Hill'48-R anisotropic coefficients of AA5754-O.

Yield criteria	F	G	H	N
Hill'48-R	0.4993	0.6377	0.3623	1.5210

**Table 3.** Barlat 1989 anisotropic coefficients of AA5754-O.

Yield criteria	a	c	h	p	M
Barlat 1989	1.2347	0.7653	1.4896	0.9747	8

**Table 4.** YLD2000-2D anisotropic coefficients of AA5754-O.

Yield criteria	$\alpha_1$	$\alpha_2$	$\alpha_3$	$\alpha_4$	$\alpha_5$	$\alpha_6$	$\alpha_7$	$\alpha_8$
YLD2000-2D	0.936	0.989	0.984	1.009	1.024	0.994	0.978	1.014

**Table 5.** Swift-Voce hardening law coefficients of Aluminum alloy grade AA5754-O sheet.

Hardening law	K	n	$\epsilon_0$	$R_{sat}$	C
Swift-Voce	396.5	0.2685	0.005954	255.2	14.75

### 2.3.1.3 YLD2000-2D yield criterion

In 2000, Barlat developed functional of yield criterion from Barlat 1989 yield criterion base on stress-3D By using the YLD2000-2d criterion, the yield function is calculated based on the linear transformation, as explained in Equation (7).

$$\phi = \phi' + \phi'' = 2\sigma^M \quad (7)$$

$\phi'$  and  $\phi''$  are the stress state that calculated by the principle deviatoric stresses as given in Equation (8).

$$\phi = f(\sigma) = |s'_1 - s'_2|^M + |2s''_2 + s''_1|^M + |2s''_1 + s''_2|^M = 2\sigma^M \quad (8)$$

Where  $S_i'$  and  $S_i''$  are the principal values of the stress tensors  $S'$  and  $S''$ . In the Equation (9)  $L'$  and  $L''$  are the coefficients.

$$\begin{pmatrix} s'_{xx} \\ s'_{yy} \\ s'_{xy} \end{pmatrix} = \begin{bmatrix} L'_{11} & L'_{12} & 0 \\ L'_{21} & L'_{22} & 0 \\ 0 & 0 & L'_{66} \end{bmatrix} \begin{pmatrix} S_{xx} \\ S_{yy} \\ S_{xy} \end{pmatrix}, \quad \begin{pmatrix} s''_{xx} \\ s''_{yy} \\ s''_{xy} \end{pmatrix} = \begin{bmatrix} L''_{11} & L''_{12} & 0 \\ L''_{21} & L''_{22} & 0 \\ 0 & 0 & L''_{66} \end{bmatrix} \begin{pmatrix} S_{xx} \\ S_{yy} \\ S_{xy} \end{pmatrix} \quad (9)$$

That involve 8 anisotropy parameters  $\alpha_1 - \alpha_8$  are given in Equation (10).

$$\begin{pmatrix} L'_{11} \\ L'_{12} \\ L'_{21} \\ L'_{22} \\ L'_{66} \end{pmatrix} = \begin{bmatrix} \frac{2}{3} & 0 & 0 \\ -\frac{1}{3} & 0 & 0 \\ 0 & -\frac{1}{3} & 0 \\ 0 & \frac{2}{3} & 0 \\ 0 & 0 & 1 \end{bmatrix} \begin{pmatrix} \alpha_1 \\ \alpha_2 \\ \alpha_7 \end{pmatrix}, \quad \begin{pmatrix} L''_{11} \\ L''_{12} \\ L''_{21} \\ L''_{22} \\ L''_{66} \end{pmatrix} = \begin{bmatrix} -2 & 2 & 8 & -2 & 0 \\ 1 & -4 & -4 & 4 & 0 \\ 4 & -4 & -4 & 4 & 0 \\ -2 & 8 & 2 & -2 & 0 \\ 0 & 0 & 0 & 0 & 9 \end{bmatrix} \begin{pmatrix} \alpha_3 \\ \alpha_4 \\ \alpha_5 \\ \alpha_6 \\ \alpha_8 \end{pmatrix} \quad (10)$$

YLD2000-2D coefficients can calculated from mechanical property of materials as indicated in Table 4.

### 2.3.2 Swift-Voce hardening law

The true stress-strain curve in plastic deformation of aluminum alloy grade AA5754-O were calculated by Swift-Voce hardening law as follows:

$$f(x) = [(1-\alpha)K(x + \epsilon_0)^n] + [\alpha(R_{sat} - (R_{sat} - R_0)e^{-Cx})] \quad (11)$$

The Swift-Voce hardening law is one of the equations that can best describe work hardening in aluminum alloy materials. Besides considering the parameters K, n, and  $\epsilon_0$ , this equation also considers the material's r-value in the hardening law equation. This allows it to effectively represent and explain the true stress-strain curve of materials exhibiting anisotropic behavior. The Swift-Voce hardening law coefficients for aluminum alloy grade AA5754-O sheet are provided in Table 5.

### 2.3.3 Failure models

#### 2.3.3.1 Keeler-Brazier original equation

In 1977, Keeler and Brazier proposed equations for creating the Forming Limit Curve (FLC), considering the values of the work hardening exponent (n) and sheet thickness (t) to determine the FLC<sub>0</sub>, which is the lowest point on the FLC. The equations devised by Keeler and Brazier are referred to as the Keeler-Brazier original equations, and they can be calculated to find the FLC<sub>0</sub> as shown in Equation (12).

$$FLC_0 = \ln \left[ 1 + \left( \frac{23.3 + 14.13t}{100} \right) \frac{n}{0.21} \right] \quad (12)$$

The left side of FLC as shown in Equations (13).

$$\epsilon_1 = FLC_0 - \epsilon_2 \quad (13)$$

The Right side of FLC as shown in Equations (14).

$$\epsilon_1 = (1 + FLC_0)(1 + \epsilon_2)^{0.5} - 1 \quad (14)$$

#### 2.3.3.2 Keeler-Brazier modified I equation

Subsequently, in 2015, Paul developed an updated version of the Keeler-Brazier equations by introducing an additional parameter, denoted as "p", into the equations. Paul's modification was based on

the observation that different types of materials have different constant values. The equations derived by Paul from the Keeler-Brazier original equations are now referred to as the "Keeler-Brazier modified I" equations. This modification resulted in changes to the right side of the FLC equations compared to the original equations, as shown in Equations (15). Despite the addition of variables for calculation purposes, the equations used to determine the  $FLC_0$  and the left side of the FLC equation remain the same as those devised by Keeler and Brazier, as shown in Equation (12) and Equation (13), respectively.

$$\varepsilon_1 = (1 + FLC_0)(1 + \varepsilon_2)^p - 1 \quad (15)$$

The constant value of the material ( $p$ ) can be calculated as shown in Equation (16).

$$p = 1.083 \text{Exp}(-1.411 \text{FLC}_0) - 0.361 \quad (16)$$

### 2.3.3.3 Anisotropic plastic deformation parameters

When considering at what point a material undergoes plastic deformation, one indicator is the yield criteria. In this research, the Hill'48-R yield criterion has been selected then consider the  $r$ -values of the material in the  $0^\circ$ ,  $45^\circ$ , and  $90^\circ$  directions concerning the rolling direction of the sheet metal, obtained from uniaxial tensile tests, to calculate the anisotropic parameters  $F$ ,  $G$ ,  $H$ , and  $N$ . The Hill'48-R anisotropic coefficients of AA5754-O are shown in Table 2. Another significant phenomenon related to plastic deformation is work hardening. One of the commonly used hardening models for aluminum alloys is the Swift-Voce hardening law, as shown in the Equation (11). When the Swift-Voce hardening law equation is used to describe the material behavior during the plastic deformation stage, it provides true stress-strain curve data, which can be utilized as data for simulating in software. The true stress-strain curves of AA5754-O material in the  $0^\circ$ ,  $45^\circ$  and  $90^\circ$  directions concerning the rolling direction of the sheet metal, fitted by the Swift-Voce hardening law equation, as depicted in Figure 2.

## 2.4 Methodology

### 2.4.1 Preparing specimen for Nakajima stretch forming test according to ISO12004

The workpiece for the Nakajima stretches forming test, prepared according to ISO12004 standards and used a wire cutting machine for preparing the specimen. The resulting workpiece is shown in Figure 3.

From the Figure 3, the specimen exhibits different shapes, representing the material receiving different stress. This subsequently

results in different strain paths in the pieces after the testing process, according to the different shapes of the specimen.

### 2.4.2 Preparing Nakajima specimen by laser marking combined with elastic paints

In this research, the material aluminum alloy grade AA5754-O was studied, and it was found that it cannot be "Electrolyte etching" according to ISO 12004 standards [13]. Therefore, the researchers conducted a literature review to find alternative methods for etching materials in the aluminum alloy group. One method found in the literature is laser marking. However, using this method for etching surfaces can lead to groove formation on the workpiece surface [36], directly affecting the forming limit curve (FLC) after the Nakajima test. Consequently, the researchers modified the laser method to ensure that laser marking does not significantly alter the material properties or FLC after testing. After numerous trial-and-error experiments, the optimal method for etching AA5754-O material was determined to be "laser marking combined with elastic coating" by laser machine as shown in Figure 4(a). This involves applying elastic coating, which has good stretching properties, to the surface to allow for deformation during the Nakajima test, similar to electrolyte etching process. The preparation process involves cleaning the workpiece surface as shown in Figure 4(b), spraying black elastic paints (Black elastic rubberized peelable; R.J. LONDON chemicals IND. Thailand) onto the desired area as shown in Figure 4(c), allowing it to dry, and then laser etching using specific patterns, as shown in Figure 4(d). Optical strain measurement devices were used to measure strain values during the process. After laser treatment with the lowest possible power to ensure the elastic paints adheres to the surface, the workpiece is coated with lacker elastic to prevent the etching from peeling off during Nakajima testing.

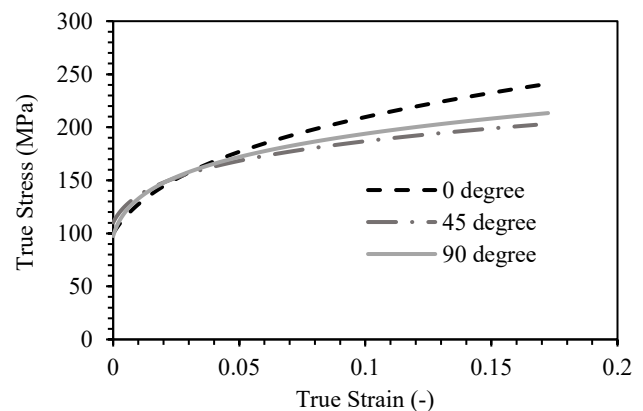


Figure 2. True stress-strain curves of AA5754-O material.

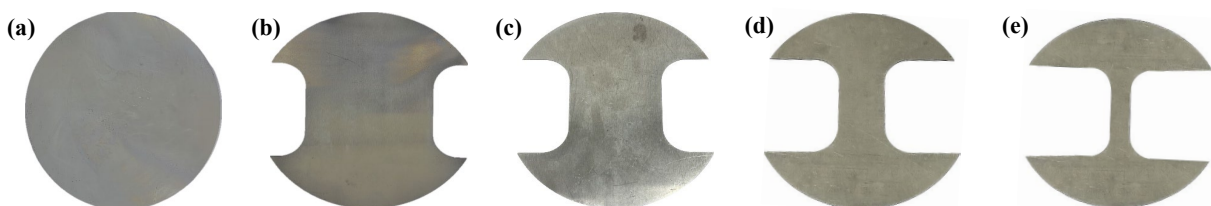
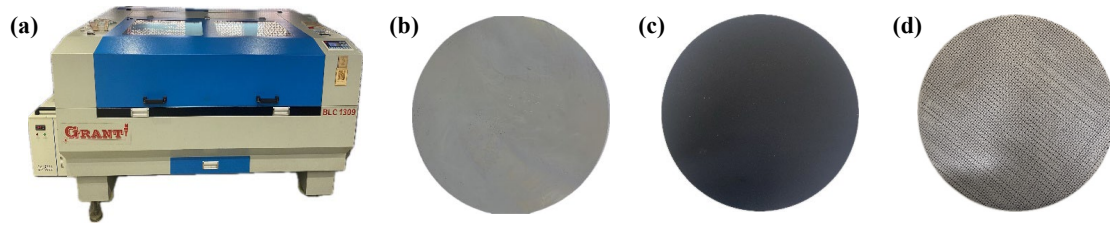
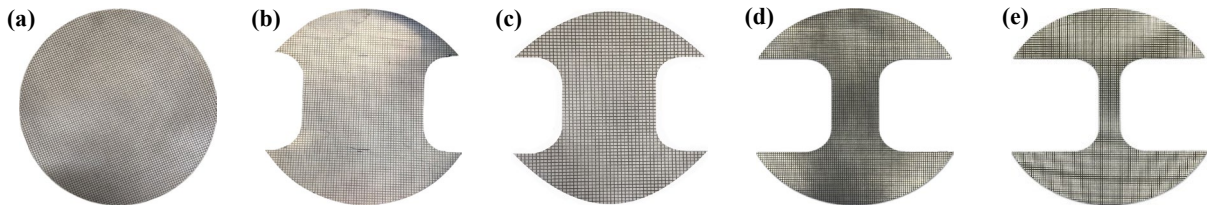


Figure 3. Specimen of Nakajima test (a) Biaxial, (b) Intermediate Biaxial, (c) Plane Strain, (d) Intermediate Uniaxial, and (e) Uniaxial.



**Figure 4.** (a) Laser Machine, (b) Specimen of Nakajima test, (c) Specimen of Nakajima test with black elastic paints, and (d) Grid from laser marking combined with elastic paints.



**Figure 5.** Grid on Nakajima specimen from laser marking combined with elastic paints.

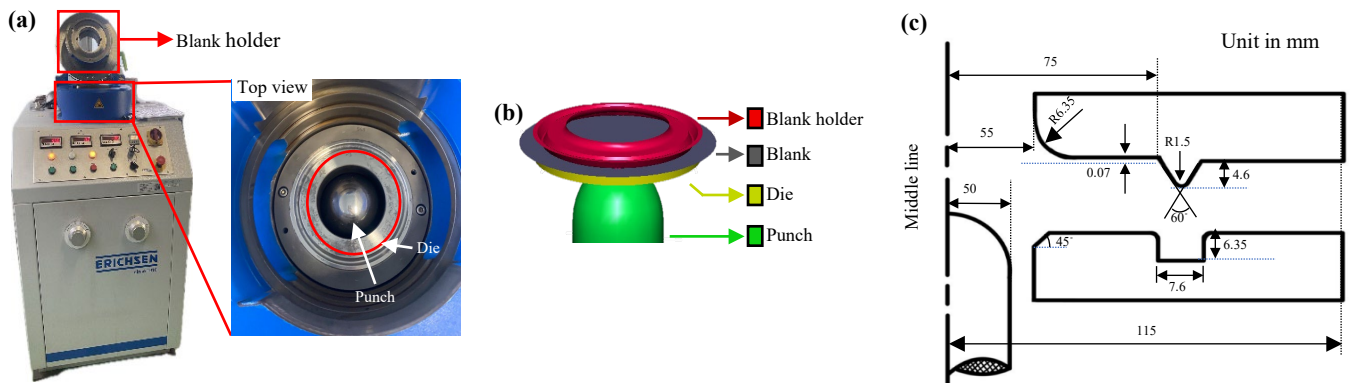


**Figure 6.** (a) Component of erichsen machine, (b) Component of Nakajima simulation and (c) Diagrammatic component of erichsen machine.

The specimens for the Nakajima test of all shapes were processed through the "Laser marking combined with elastic paints" method, as shown in Figure 5.

### 2.4.3 Finite element analysis simulation

#### 2.4.3.1 Nakajima stretch forming test simulation according to ISO 12004

The Nakajima stretch forming test was conducted using the erichsen machine, as depicted in Figure 6(a) and adhered to the testing conditions specified in the ISO12004 standard. Additionally, the test was simulated using the PAM-STAMP software, utilizing parameters obtained from the actual tests conducted at the iron and steel institute of Thailand, as illustrated in the accompanying Figure 6(b).

#### 2.4.3.2 Forming fuel tank of motorcycle part by deep drawing process

In this research, the forming process of the motorcycle fuel tank component made from AA5754-O was simulated using the PAM-STAMP program. The simulation consists of several components, including the blank, die, punch, and blank holder, as depicted in

Figure 7(b). For the simulation process, it was essential to input material data in the form of a true stress-strain curve, obtained by fitting the equation of the Swift-Voce hardening law. This curve characterizes behavior of the sheet metal material during the deep drawing process. Another crucial aspect of the simulation was the determination of whether the sheet metal material under study would experience damage or failure. This determination is made through the FLC. The forming process simulation is referenced to actual process forming simulations, as illustrated in Figure 7(a).

## 3. Results and discussion

### 3.1 Measurement grid size from laser marking combined with elastic paints method

In this research, an experimental study was conducted using a novel process that had not been previously used: "Laser marking combined with elastic paints". Subsequently, the grid on the surfaces of the Nakajima specimen was measured for true major strain values before subjecting them to the Nakajima stretch forming test. This was done to assess the uniformity of the etching produced by the new process, as illustrated in the accompanying Figure 8.

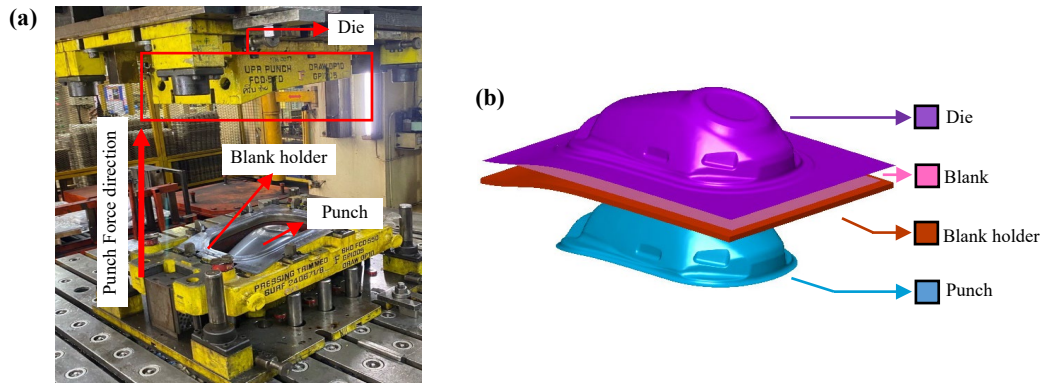


Figure 7. (a) Component of motorcycle fuel tank in actual production, and (b) Component of fuel tank part in deep drawing process simulation

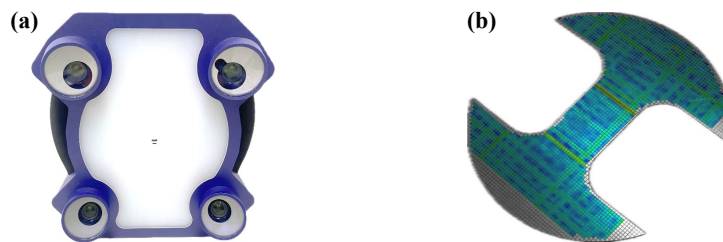


Figure 8. (a) Optical strain measurement system, and (b) Strain of specimen before testing.

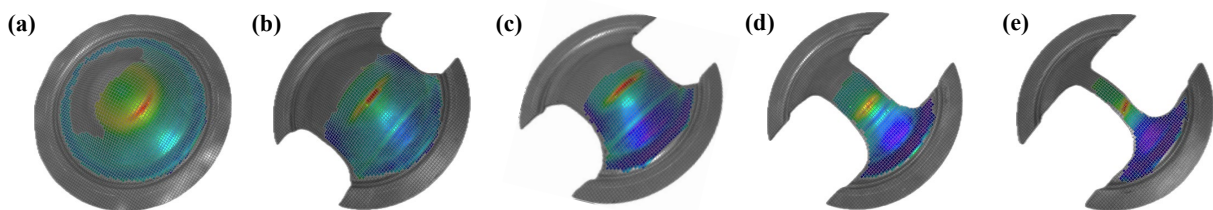


Figure 9. Result of strain after Nakajima test using optical strain measurement system (a) biaxial, (b) intermediate biaxial, (c) plane strain, (d) intermediate uniaxial, and (e) uniaxial.

From Figure 8, it is evident that the grid produced by the laser marking combined with the elastic paints process exhibits the highest true major strain value of only 0.04 on the workpiece. This etching is considered the best, as it does not result in any defects on the aluminum workpiece. The observed etching is merely a layer of black elastic paints, which can be easily removed without causing any damage or changing the mechanical property of the workpiece.

### 3.2 Forming limit curves

In this study, obtaining the forming limit curve from two processes: the Nakajima stretch forming test and the materials model.

#### 3.2.1 Forming limit curves from Nakajima test

After subjecting the workpiece prepared according to the ISO12004 standard to forming using an Erichsen machine until damage occurred, the condition of the damaged workpiece is illustrated in Figure 9.

After that, the workpiece was subjected to reading the true major strain and true minor strains using the optical strain measurement

system model AsutoGrid Vialux, as shown in Figure 8(a). Different colors indicate varying strain values on the different parts of the damaged workpiece, with the red areas indicating the highest strain. Then, data from the Nakajima test, as depicted in Figure 10(a), were selected. Finally, a forming limit curve was generated based on this data, as shown in Figure 10(b).

From Figure 10(b), it can be observed that the forming limit curve (FLC) was not generated from the position of the data where the highest strain occurred in Figure 10(a). This is because, in this research, the occurrence of localized necking on the sheet metal in the forming process indicates material damage. Therefore, the data selected for FLC generation, considering the occurrence of localized necking, were collected from rows 3 to 4, next to the position where the fracture occurred on the Nakajima test workpiece.

#### 3.2.2 Forming limit curves from materials model

In this research, the FLC obtained from the materials model was derived using the equations of the Keeler-Brazier modified I, represented by a blue line graph as shown in Figure 11.

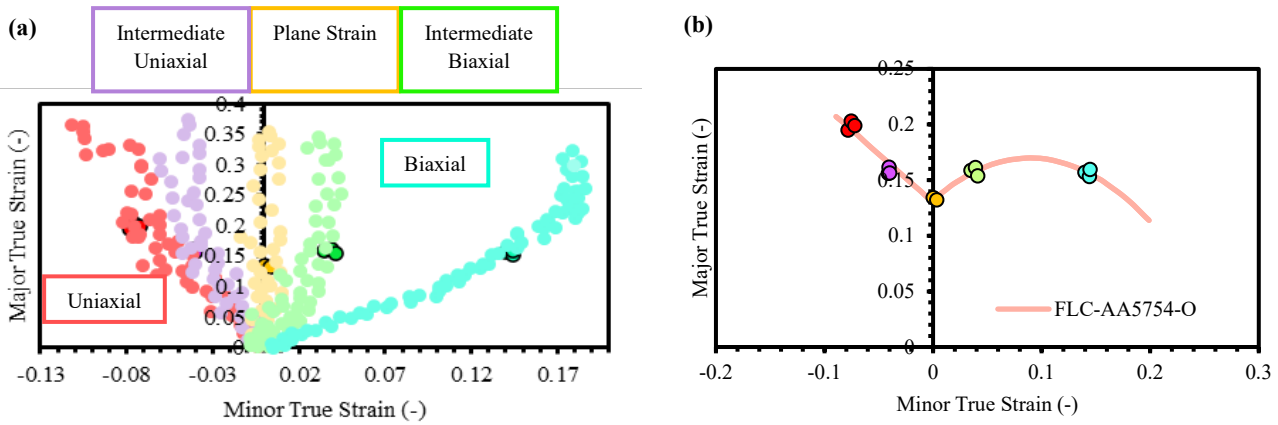


**Figure 10.** (a) Raw data of true major-minor strains of Nakajima specimen, and (b) Selected localized necking data for generate FLC.

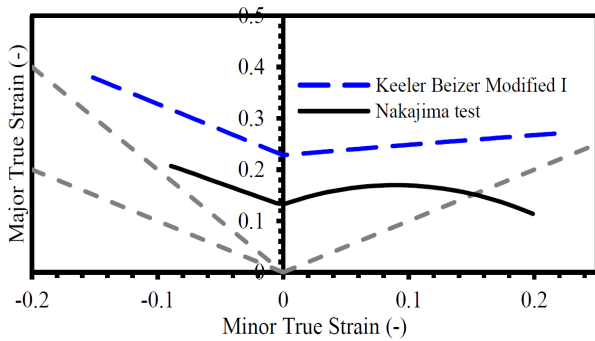


**Figure 11.** Forming limit curve by Materials model

From the Figure 11, the FLC from the Nakajima stretch forming test has the lowest FLC<sub>0</sub> point. This is because the focus of this study is on collecting data occurrence of localized necking behavior because product will be failure that this behavior appears. When comparing the FLC from the experimental data with the FLC from the Keeler-Brazier modified I equation, it can be observed that the right side of the FLC curve from the Keeler-Brazier modified I equation is slightly less curved compared to the FLC from the experimental data.

### 3.3 Nakajima stretch forming test using finite element analysis simulation

The comparison between the positions of fractures on the Nakajima test specimens during actual testing and simulation using the PAM-STAMP software, where different yield criteria and FLCs are applied, results in variations in the strain paths experienced by the workpiece post-testing. These variations directly impact the locations where damage occurs after the testing process. Figure 12 depicts the locations

of fractures occurring on the Nakajima test specimens in all five patterns in actual testing.

In simulating the Nakajima test using different yield criteria such as Hill 1948, Barlat 1989, and YLD2000-2D yield criteria, the positions of fractures occurring on the test specimens in all five patterns after testing are depicted in Figure 13.

From Figure 13, it is evident that the positions of damage occurring on the Nakajima test specimens differ when using different yield criteria, namely Hill 1948, Barlat 1989, and YLD2000-2D. When comparing these positions to the actual test results, it is observed that there are similar positions of fractures, except in the case of the uniaxial specimen. In the simulation, there are two different fracture positions compared to the actual specimen, which has only one fracture position. Moreover, the fractures simulated using the three different yield criteria show positions that are relatively close to each other, although the sizes of the fractures differ. Notably, when using the YLD2000-2D yield criterion for simulating the Nakajima test in the PAM-STAMP software, the positions of fractures closely resemble the actual testing results. This is because the positions of fractures simulated using all three yield criteria for representative strain paths, such as plane strain, intermediate uniaxial, and uniaxial specimens, are very close to each other. Therefore, the comparison of fracture positions on biaxial and intermediate biaxial specimens from Figure 13 reveals that only the YLD2000-2D yield criterion can accurately predict fracture positions closest to reality. Using the Hill 1948 yield criterion results in very small fractures on the biaxial specimen, which do not closely match the actual test. Meanwhile, the Barlat 1989 yield criterion leads to fractures occurring only on one side of the intermediate biaxial specimen, which does not align with the actual testing. Thus, it can be concluded that using the YLD2000-2D yield criterion provides simulation results that closely resemble the actual testing conditions.

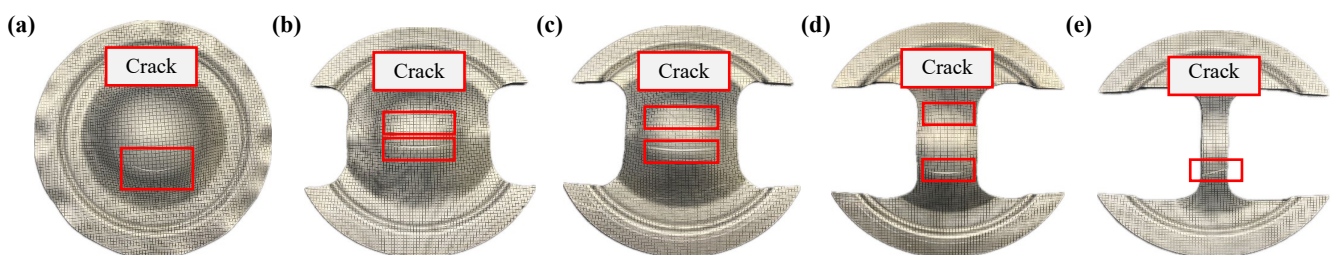


**Figure 12.** Position of cracking on Nakajima specimens after testing (a) biaxial, (b) intermediate biaxial, (c) plane strain, (d) intermediate uniaxial, and (e) uniaxial

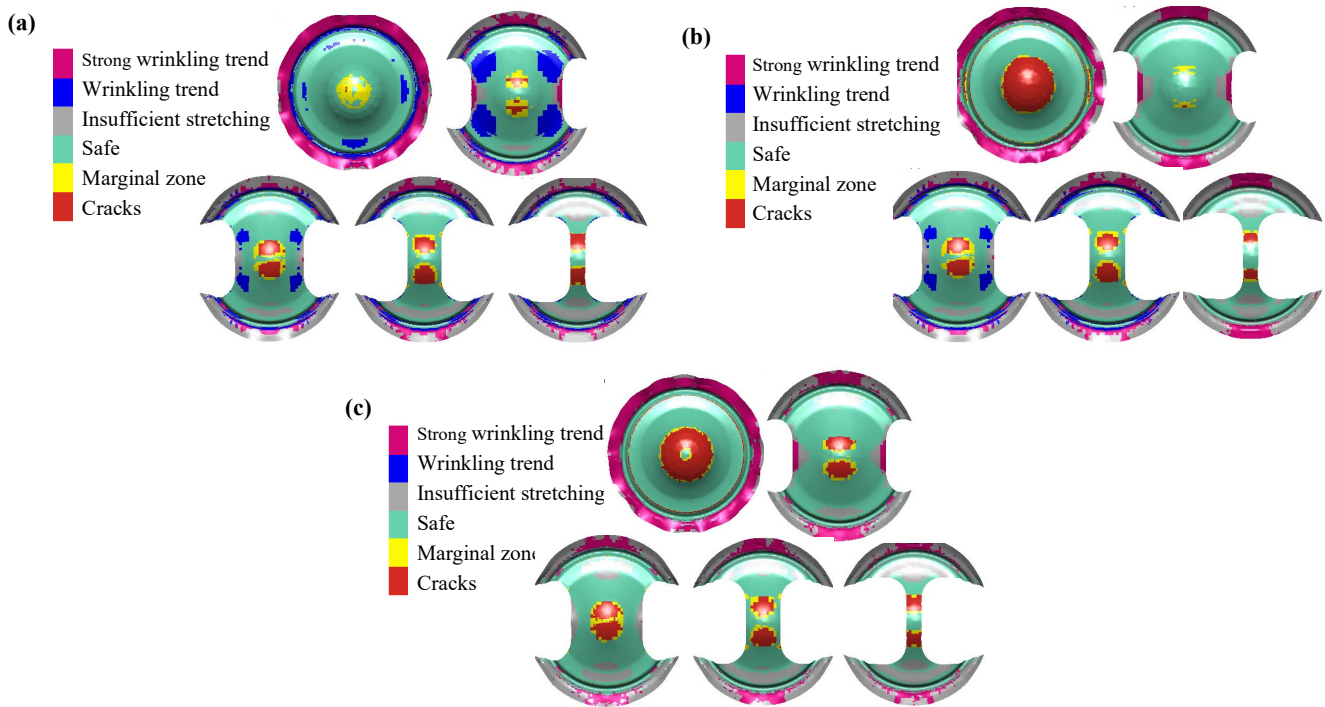


**Figure 13.** Position of cracking on Nakajima specimens after simulation in PAM-STAMP program using: (a) Hill 1948 yield criterion, (b) Barlat 1989 yield criterion, and (c) YLD2000-2D yield criterion.

### 3.4 Position of cracking between actual process and finite element analysis simulation

In this research, the deep drawing process of the fuel tank component made from aluminum alloy grade AA5754-O has been simulated under conditions similar to actual production in the industry. This simulation was conducted using the PAM-STAMP software. The forming limit curve (FLC) from the Nakajima stretch forming test and materials models were utilized to predict the positions of cracks on the product after the deep drawing process.

#### 3.4.1 Simulation results

##### 3.4.1.1 Using forming limit curve from Nakajima stretch forming test

When using the FLC from the Nakajima stretch forming test to predict the position of cracking or failure in PAM-STAMP, as shown in Figure 14(a). In this research, the ability to effectively predict fracture behavior in the deep drawing process of AA5754-O material is partly due to the use of “Fully automatic surface meshing integrated by Delta MESH” in the PAM-STAMP program. This meshing technique, developed by ESI Group, is employed to create the mesh of material sheet before simulating the forming process of motorcycle fuel tank parts. The simulation results are using the FLC of the Nakajima test, which was used as a reference to validate because it received the actual testing.

From the Figure 14(a), it depicts the fuel tank of a motorcycle after the deep drawing process. The red-colored area on the workpiece indicates the region where cracking or damage has occurred. Meanwhile, the yellow-colored area represents the region with a risk of potential

damage after the forming process. Regarding the Figure 14(b), it illustrates the strain path that occurs on the aluminum alloy grade AA5754-O sheet after the forming process under conditions similar to actual production. If the strain path on the workpiece exceeds the value of the FLC, damage will occur.

##### 3.4.1.2 Using forming limit curve from Keeler-Beizer modified I

When using forming limit curve from Keeler-Beizer modified I for predicting position of cracking or failure in PAM-STAMP, as shown in Figure 15(a).

From the Figure 15(a), the red area on the workpiece indicates the region where cracking or damage occurs, while the yellow area represents the region at risk of damage after the forming process. As for the Figure 15(b), it illustrates the strain path experienced by the material after the forming process under conditions identical to actual production. It can be observed that the FLC of the Keeler-Brazier modified I is higher than the FLC obtained from the Nakajima test, which makes the number of cracks on the product after the forming process less than when compared with the FLC of the Nakajima test.

### 3.4.2 Comparison position of cracking between actual process and finite element analysis simulation

After simulating the deep drawing process of the fuel tank component made from aluminum alloy grade AA5754-O, there will be validation of the crack positions post-forming on the product by comparing the simulation results using the forming limit curve (FLC) with the actual forming process in the industry under the same forming conditions. This is depicted in Figure 7(a).

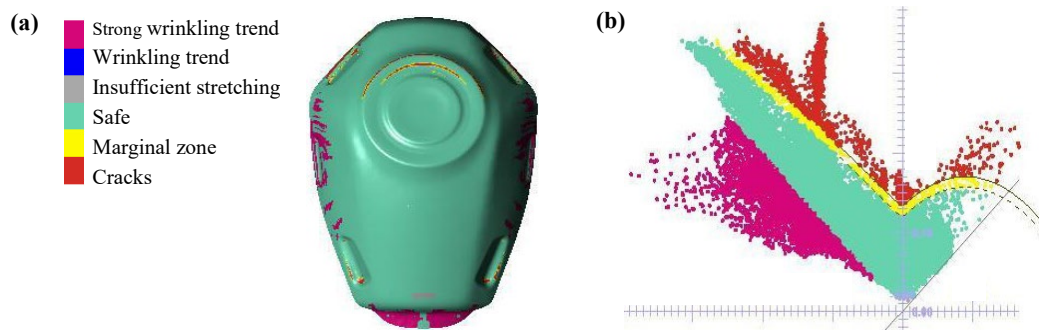


**Figure 14.** (a) Results of deep drawing simulation using FLC from Nakajima test, and (b) Strain path on specimen using FLC from Nakajima test.

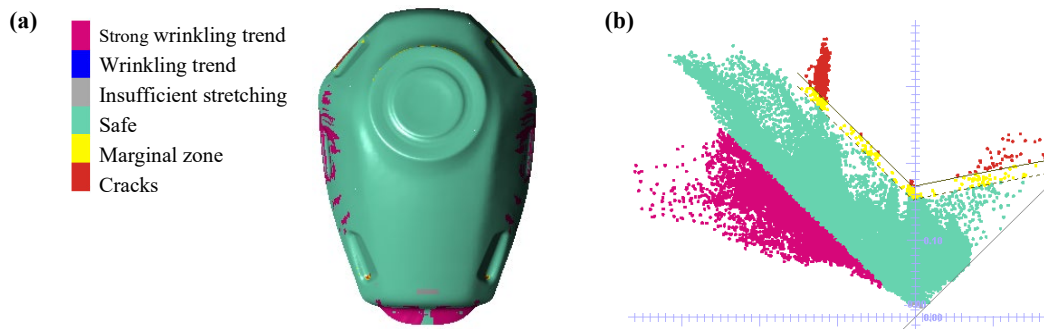


**Figure 15.** (a) Results of deep drawing simulation using FLC from Keeler- Brazier modified I, and (b) Strain path of specimen using FLC from Keeler-Brazier modified I equation

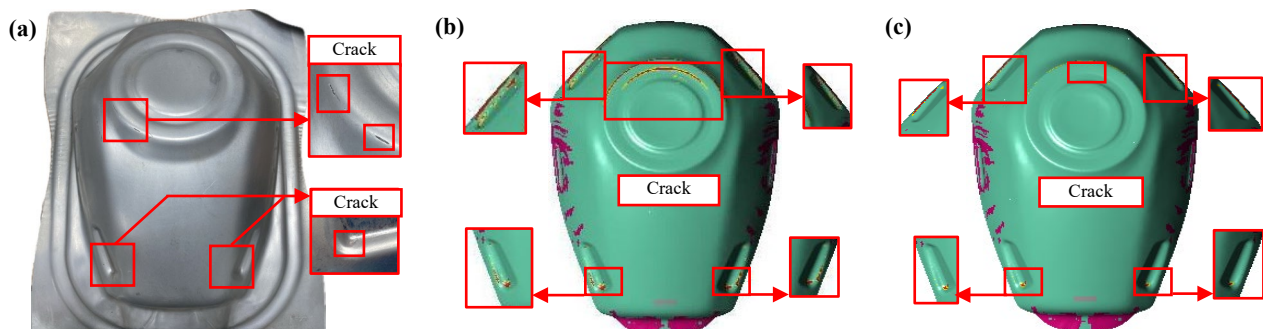


**Figure 16.** Position of cracking on fuel tank of motorcycle (a) Actual forming process, (b) Simulation using FLC of Nakajima test, and (c) Simulation using FLC of Keeler-Brazier modified I.

When comparing the positions of cracking on the motorcycle fuel tank product between using the FLC of the Nakajima stretch forming test and the FLC of the Keeler-Brazier modified I with the position of cracking on the fuel tank of the motorcycle in the actual process, as shown in Figures 16(a-c), respectively. It can be observed that using the FLC from the Nakajima test to predict the position of damage results in more occurrences of cracking compared to using the FLC from the Keeler-Brazier modified I equation because, in this research, it is considered that when localized necking behavior occurs on the workpiece, it indicates that damage has already occurred. When comparing the crack patterns between simulations using the FLC from the Nakajima test and the actual manufacturing process, it is found that using the FLC from the Nakajima test results in more cracks occurring in the simulation than in the actual forming process. This is because in the actual production, the post-formed workpiece can clearly show visible damage, namely cracks, without examining whether there are areas at risk of damage, such as occurrences of

localized necking or small cracks that are not visible to the naked eye. On the contrary, in simulations using the FLC, it is possible to identify the positions at risk of damage and crack occurrences, including small cracks that are not visible to the human eye. This is one of the reasons why using the FLC to predict the positions of damage in simulations results in more damaged areas on the product than in actual production.

#### 4. Conclusions

In this work, a new method for creating a grid on Nakajima workpieces, which is similar to the grid creation process using electrolyte-etching and the FLC of aluminum alloy sheet AA5754-O, has been generated by two processes: experimental Nakajima stretch forming tests according to ISO 12004 and a materials model. These were then used with FLC from the experimental and materials models to predict the locations of potential damage to fuel tank workpieces after deep drawing processes. The study compared three yield criteria

models: Hill's 1948 R-approach, Barlat 1989, and the YLD2000-2D yield criterion, to predict the positions of damage on workpieces following Nakajima test simulations. This was done to select the most suitable yield criteria to be used alongside the Swift-Voce hardening law and Keeler-Brazier modified I for generating the FLC from the materials model. The significant findings from this investigation are summarized in the following bullet points:

Due to difficulties encountered in creating a grid using electrolyte etching for Nakajima stretching forming tests according to ISO12004, a new method was devised. This method involves laser marking combined with elastic color. The grid on the workpiece created through this process consists of a layer of elastic paint, which can be removed without affecting the mechanical properties of the material for subsequent testing processes. Additionally, workpieces grid-marked with this new method were inspected using the optical strain measurement system model AsutoGrid Vialux, which measured strain values and ensured a highly uniform grid size.

When comparing the three yield criteria models: Hill's 1948 R-approach, Barlat 1989, and the YLD2000-2D yield criterion, regarding their impact on the location of damage on workpieces after simulating Nakajima tests, it can be concluded that the use of the YLD2000-2D yield criterion can predict the positions of damage on workpieces in Nakajima test simulation by the PAM-STAMP program, which closely reflects the position of failure on automotive parts in the actual forming process.

From generating the FLC using the Keeler-Brazier modified I equation combined with the YLD2000-2D yield criterion and Swift-Voce hardening law in the PAM-STAMP program to predict failure on motorcycle fuel tank parts after the deep drawing process, compared to predicting failure using the FLC from Nakajima tests, it can be summarized that the FLC from Nakajima tests is lower and has a greater curvature on the right side compared to the FLC of the Keeler-Brazier modified I equation.

When comparing the positions of damage on motorcycle fuel tanks after the deep drawing process between actual forming and simulations in PAM-STAMP using the FLC from Nakajima tests and the FLC of the Keeler-Brazier modified I equation, it is observed that the use of the FLC from the Materials model employed in this research accurately predicts the locations of damage on the workpieces when compared to real-world industrial components. Even though the FLC from experiments predicts that the workpieces will experience a certain number of cracks after the forming process due to the data collection during localized necking behavior, the use of FLC from the experimental work in this study predicts that there will be more damage-prone areas than when using the FLC from the Materials model.

Finally, from this research, by using the Keeler-Brazier modified I equation to construct the forming limit curve in conjunction with YLD2000-2D and the Swift-Voce hardening law for aluminum alloy materials for the first time, it can be concluded that when applying Keeler-Brazier modified I to predict the behavior of AA5754-O sheet metal used in motorcycle fuel tank parts in the PAM-STAMP software, the locations of fractures on the fuel tank parts predicted by Keeler-Brazier modified I closely match those observed in actual industrial forming processes and those predicted by the FLC from the Nakajima test. While the regions of damage are consistent across all methods, the size of the fractures differs. Although the FLC from the Nakajima

test, when used in simulations, results in more extensive post-forming damage compared to the FLC from Keeler-Brazier modified I and actual industrial forming processes, this discrepancy arises because the Nakajima test collects data below the fracture point, specifically in areas where the material experiences "necking". In industrial applications, necking is considered indicative of part failure. In contrast, when comparing only the locations of damage on parts formed in actual industrial processes with simulations using the FLC by Keeler-Brazier modified I, the positions of the damage and the extent of the damage are very similar. Thus, applying Keeler-Brazier modified I to construct the FLC in conjunction with YLD2000-2D and the Swift-Voce hardening law for aluminum alloy materials accurately predicts the forming behavior of AA5754-O sheet metal in the production of fuel tank parts through the deep drawing process. This method shows high accuracy when compared with parts formed in the automotive manufacturing industry.

## Acknowledgement

The authors would like to express their gratitude for the financial support received through the Petchra Pra Jom Klao Master's Degree and Ph.D. Research Scholarship from King Mongkut's University of Technology Thonburi. They also sincerely thank THAI SUMMIT GOLD PRESS THAILAND for supporting material AA5754-O and fuel tank parts in the research study.

## References

- [1] S. Das, A. Engineering, and C. Analyst, "Design and weight optimization of aluminium alloy wheel," *International Journal of Scientific and Research Publications*, vol. 4, no. 6, 2014.
- [2] C. Author, "ORIGINAL ARTICLES Magnesium and Aluminum Alloys in Automotive Industry," 2012. [Online]. Available: <http://www.worldaluminium.org>.
- [3] M. Fadzli Abdollah, and R. Hassan, "Preliminary design of side door impact beam for passenger cars using aluminium alloy", *Journal of Mechanical Engineering and Technology*, vol. 5, no. 1, 2010.
- [4] B. Ma, C. Yang, X. Wu, and L. Zhan, "Theoretical and numerical investigation of the limit strain of a 5754-O aluminum alloy sheet considering the influence of the hardening law," *Journal Materials Engineering and Performance*, vol. 32, pp. 10115-10127, 2023.
- [5] Q. Hu, and J. W. Yoon, "The roles of yield function and plastic potential under non-associated flow rule for formability prediction with perturbation approach," in *IOP Conference Series: Materials Science and Engineering*, IOP Publishing Ltd, 2020.
- [6] M. Türköz, Ö. N. Cora, H. Gedikli, M. Dilmeç, H. S. Halkacı, and M. Koç, "Numerical optimization of warm hydromechanical deep drawing process parameters and its experimental verification," *Journal of Manufacturing Processes*, vol. 57, pp. 344-353, 2020.
- [7] M. Tinkir, M. Dilmeç, M. Türköz, and H. S. Halkacı, "Investigation of the effect of hydromechanical deep drawing process parameters on formability of AA5754 sheets metals by using neuro-fuzzy forecasting approach," *Journal of Intelligent & Fuzzy Systems*, vol. 28, pp. 647-659, 2015.

- [8] W. Yuan, M. Wan, and X. Wu, "Prediction of forming limit curves for 2021 aluminum alloy," in *Procedia Engineering*, Elsevier Ltd, 2017, pp. 544-549.
- [9] T. K. Hoang, T. T. Luyen, and D. T. Nguyen, "Enhancing/improving forming limit curve and fracture height predictions in the single-point incremental forming of Al1050 sheet material," *Materials*, vol. 16, no. 23, 2023.
- [10] R. Zhang, Z. Shao, and J. Lin, "A review on modelling techniques for formability prediction of sheet metal forming," *International Journal of Lightweight Materials and Manufacture*, vol. 1, no. 3, pp. 115-125, 2018.
- [11] X. Zhan, Z. Wang, M. Li, Q. Hu, and J. Chen, "Investigations on failure-to-fracture mechanism and prediction of forming limit for aluminum alloy incremental forming process," *Journal of Materials Processing Technology*, vol. 282, 2020.
- [12] Y. Dewang, M. S. Hora, and S. K. Panthi, "Prediction of crack location and propagation in stretch flanging process of aluminum alloy AA-5052 sheet using FEM simulation," *Transactions of Nonferrous Metals Society of China (English Edition)*, vol. 25, no. 7, pp. 2308-2320, 2015.
- [13] "ISO 12004-2 Metallic materials – Sheet and strip – Determination of forming-limit curves. Part 2: Determination of forming-limit curves in the laboratory," in *ISO 12004-2*, 2008.
- [14] M. Tomáš, E. Evin, S. Németh, and J. Hudák, "Evaluation of limit deformations of zn coated high strength steel," in *Materials Science Forum*, vol. 818, pp. 248-251, 2015.
- [15] V. A. M. Cristino, M. B. Silva, P. K. Wong, and P. A. F. Martins, "Determining the fracture forming limits in sheet metal forming: A technical note," *Journal of Strain Analysis for Engineering Design*, vol. 52, no. 8, pp. 467-471, 2017.
- [16] K. Mäntyjärvi, J. Tulonen, T. Saarnivuo, J. Porter, and J. A. Karjalainen, "Grid patterns by laser for forming strain analysis," *International Journal of Material Forming*, vol. 1, no. 1, pp. 249-252, 2008.
- [17] X. Li, Y. Chen, L. Lang, and R. Xiao, "A modified m-k method for accurate prediction of flc of aluminum alloy," *Metals (Basel)*, vol. 11, no. 3, pp. 1-12, 2021.
- [18] Z. Q. Sheng, and P. K. Mallick, "Predicting sheet forming limit of aluminum alloys for cold and warm forming by developing a ductile failure criterion," in *Journal of Manufacturing Science and Engineering, Transactions of the ASME*, American Society of Mechanical Engineers (ASME), 2017.
- [19] P. Larpprasoetkun, J. Leelaseat, A. Nakwattanaset, A. Sunanta, and S. Suranuntchai, "Study on the material models of the forming limit curves development for predicting a fracture behavior of AA5754-O in automotive parts," *Key Engineering Materials*, vol. 973, pp. 81-86, 2024.
- [20] S. Panich, F. Barlat, V. Uthaisangsuk, S. Suranuntchai, and S. Jirathearanat, "Experimental and theoretical formability analysis using strain and stress based forming limit diagram for advanced high strength steels," *Materials and Design*, vol. 51, pp. 756-766, 2013.
- [21] A. L. Gurson, "Continuum theory of ductile rupture by void nucleation and growth: Part I-Yield criteria and flow rules for porous ductile media," 1977. [Online]. Available: <http://asme.org/terms>
- [22] S. K. Paul, "Controlling factors of forming limit curve: A review," *Advances in Industrial and Manufacturing Engineering*, vol. 2. Elsevier B.V., May 01, 2021.
- [23] S. K. Paul, "Path independent limiting criteria in sheet metal forming," *Journal of Manufacturing Processes*, vol. 20, pp. 291-303, 2015.
- [24] S. Panich, S. Suranuntchai, S. Jirathearanat, and V. Uthaisangsuk, "A hybrid method for prediction of damage initiation and fracture and its application to forming limit analysis of advanced high strength steel sheet," *Engineering Fracture Mechanics*, vol. 166, pp. 97-127, 2016.
- [25] A. Nakwattanaset, S. Panich, and S. Suranuntchai, "Formability prediction of high-strength steel sheet using experimental, analytical and theoretical analysis based on strain and stress forming limit curves and its application to automotive forming parts: Vorhersage der Umformbarkeit von hochfesten Stahlblechen mittels experimenteller, analytischer und theoretischer Analyse auf der Grundlage von Grenzformänderungskurven für Dehnungen und Spannungen und ihre Anwendung auf die Umformung von Automobilteilen," *Materwiss Werksttech*, vol. 54, no. 9, pp. 1122-1137, 2023.
- [26] R. Hill, "A theory of the yielding and plastic flow of anisotropic metals," 1948.
- [27] J. Lian, F. Barlat, and B. Baudelet, "Plastic behaviour and stretchability of sheet metals. part II: Effect of yield surface shape on sheet forming limit," *International Journal of Plasticity*, vol 5, no. 2, pp. 131-147, 1989.
- [28] D. Banabic, T. Balan, and D. S. Comsa, "A new yield criterion for orthotropic sheet metals under plane-stress conditions." *International Journal of Mechanical Sciences*, vol. 45, no. 5, pp. 797-811, 2003.
- [29] C. C. Roth, and D. Mohr, "Effect of strain rate on ductile fracture initiation in advanced high strength steel sheets: Experiments and modeling," *International Journal of Plasticity*, vol. 56, pp. 19-44, 2014.
- [30] I. Jang, G. Bae, J. Song, H. Kim, and N. Park, "Fracture envelopes on the 3D-DIC and hybrid inverse methods considering loading history," *Materials & Design*, vol. 194, p. 108934, 2020.
- [31] K. S. Pandya, C. C. Roth, and D. Mohr, "Strain rate and temperature dependent plastic response of AA7075 during hot forming," in *IOP Conference Series Materials Science and Engineering*, vol. 651, no. 1, p. 012100, 2019.
- [32] H. Shang, C. Zhang, S. Wang, and Y. Lou, "Large strain flow curve characterization considering strain rate and thermal effect for 5182-O aluminum alloy," *International Journal of Material Forming*, vol. 16, no. 1, 2023.
- [33] ASTM E8, "Standard Test Methods for Tension Testing of Metallic Materials," in *American Association State Highway and Transportation Officials Standard*, 2016.
- [34] S. Fang, X. Zheng, G. Zheng, B. Zhang, B. Guo, and L. Yang, "A new and direct r-value measurement method of sheet metal based on multi-camera dic system," *Metals (Basel)*, vol. 11, no. 9, 2021.

- [35] M. Ghosh, A. Miroux, and L. A. I. Kestens, "Correlating r-value and through thickness texture in Al-Mg-Si alloy sheets," *Journal of Alloys and Compounds*, vol. 619, pp. 585-591, 2015.
- [36] K. Mäntyjärvi, J. Tulonen, T. Saarnivuo, J. Porter, and J. A. Karjalainen, "Grid patterns by laser for forming strain analysis," *International Journal of Material Forming*, vol. 1, no. 1, pp. 249-252, 2008.